complexes. The latter tends to give cleaner reactions since those of the former are complicated by redox processes and ligand reactions.

Acknowledgment. Support by the Petroleum Research Fund under grant 21013-AC3 and the Tulane University Chemistry Department is gratefully acknowledged.

Supplementary Material Available: For 1, 2, 4, 7, and 8, full tables of interatomic distances, interbond angles, calculated hydrogen atom positions, anisotropic thermal parameters, and rms amplitudes of anisotropic displacement (36 pages). Ordering information is given on any current masthead page.

OM920432L

Transition-Metal Derivatives of the Cyclopentadienylphosphine Ligands. 7. Electrochemical Oxidation of $[Rh(\mu\text{-}C_5H_4PPh_2)(CO)]_2$ and Rereduction: An ECE Process Including a Fast Reversible Configurational Switch

Jean-Bernard Tommasino, Dominique de Montauzon, Xiadong He, André Maisonnat, and René Poilblanc*

Laboratoire de Chimie de Coordination du CNRS, UPR 8241 liée par conventions à l'Université Paul Sabatier et à l'Institut National Polytechnique de Toulouse, 205 Route de Narbonne, 31077 Toulouse Cedex, France

Jean-Noel Verpeaux and Christian Amatore*

Ecole Normale Supérieure, Département de Chimie, URA CNRS 1110, 24 Rue Lhomond, 75231 Paris Cedex 05, France

Received June 17, 1992

The electrochemical oxidation of the cyclopentadienylphosphine-bridged complex $[Rh(\mu\text{-}C_5H_4PPh_2)(CO)]_2$ and the reduction of the dicationic parent compound $[Rh(\mu\text{-}C_5H_4PPh_2)(CO)]_2^{2+}$ have been performed at various scan rates from 0.1 to 1200 $V \cdot s^{-1}$ using ultramicroelectrodes. The analysis of the voltammograms and their digital simulation reveal an ECE process where the intervening chemical step is a very fast reversible conformational change ($k_1 = 4000\ s^{-1}$; $k_{-1} = 2000\ s^{-1}$) involving two monocationic intermediates assumed to be respectively a non-metal–metal-bonded mixed-valence complex and a metal–metal-bonded complex (with a bond order closed to 0.5). The high rates of this conformational change, pictured as a disrotatory deformation of the $(\mu\text{-}C_5H_4PPh_2)_2$ central unit, point out to an interesting specificity of this bridging ligand.

Introduction

The hypothesis that two metals kept in close proximity could react cooperatively with substrate molecules has initiated a very broad interest in ligand systems able to lock two metal centers in such a position. As far as the chemistry of low oxidation state transition metals is concerned, tertiary diphosphines have been the most commonly employed ligands; also very short linkages are obtained with four-electron bridging units like for instance the phosphido ($\mu\text{-}PR_2^-$) and the thiolato ($\mu\text{-}SR^-$) anions. The extensive development of the chemistry of metal cyclopentadienyl derivatives and their remarkable properties led us and others to investigate the potentialities, as bridging units, of the heterodifunctional ligands containing a cyclopentadienyl ring,[1a-h] directly linked to a phosphine ligand as in the (diphenylphosphino)cyclopentadienyl anion ($^-C_5H_4PPh_2$) or by a molecular chain as in the (diphenylphosphino)ethylcyclopentadienyl anion ($^-C_5H_4(CH_2)_2PPh_2$). Such ligands are expected to tailor coordination spheres containing both cyclopentadienyl and phosphine ligands either in monometallic chelated species[1h] or in bimetallic bridged species.[1a-g,i] Our recent work on the reactions concerning oxidative addition to the dinuclear ((diphenylphosphino)cyclopentadienyl)rhodium(I) and -iridium(I) complexes $[M^I(\mu\text{-}C_5H_4PPh_2)(CO)]_2$ (M = Rh (1), Ir) has emphasized the quite novel function of the $[\mu\text{-}C_5H_4PR_2]$ bridging unit, working as a "ball and socket joint" between the two molecular moieties.[1i] Thus, this type of flexibility makes the ligand able to accommodate very different metal–metal separations, i.e., from 4.3029 Å in 1 to around 2.7 Å in various types of Rh^{II}–Rh^{II} metal–metal-bonded complexes (2.7796 Å in $[Rh^{II}(\mu\text{-}C_5H_4PPh_2)(\text{pyridine})]_2^{2+}$ (3); 2.7319 Å in $[(COCH_3)Rh^{II}(\mu\text{-}C_5H_4PPh_2)_2Rh^{II}(CO)]^+$ (4); 2.7160 Å in $[(H_3C)Rh^{II}(\mu\text{-}C_5H_4PPh_2)_2Rh^{II}(I)]$ (5)). It has therefore been inferred that the parent dicationic d^7–d^7 complexes $[M^{II}(\mu\text{-}C_5H_4PPh_2)(CO)]_2^{2+}$ (M = Rh (2), Ir) obtained by oxidation of 1 or of the iridium analog, using ferrocenium tetrafluoroborate or silver hexafluorophosphate as oxidizing reagents, offer the same prototypal structure. This was confirmed from the spectroscopic NMR and IR data. In short, the two-electron redox chemically reversible transformation leading from 1 to the dicationic derivative 2

(1) (a) Bullock, M. R.; Casey, C. P. *Acc. Chem. Res.* **1987**, *20*, 167. (b) He, X. D.; Maisonnat, A.; Dahan, F.; Poilblanc, R. *Organometallics* **1987**, *6*, 678–680. (c) Raush, M. D.; Craig Spink, W.; Atwood, J. L.; Baskar, A. J.; Bott, S. G. *Organometallics* **1989**, *8*, 1627–1631. (d) He, X. D.; Maisonnat, A.; Dahan, F.; Poilblanc, R. *Organometallics* **1989**, *8*, 2618–2626. (e) He, X. D.; Maisonnat, A.; Dahan, F.; Poilblanc, R. *J. Chem. Soc., Chem. Commun.* **1990**, 670–671. (f) Anderson, G. K.; Lin, M.; Chiang, M. Y. *Organometallics* **1990**, *9*, 288–289. (g) He, X. D.; Maisonnat, A.; Dahan, F.; Poilblanc, R. *New J. Chem.* **1990**, *14*, 313–315. (h) Kettenbach, R. T.; Butenschön, H. *New J. Chem.* **1990**, *14*, 599–601. (i) He, X. D.; Maisonnat, A.; Dahan, F.; Poilblanc, R. *Organometallics* **1991**, *10*, 2443–2445.

0276-7333/92/2311-4150$03.00/0

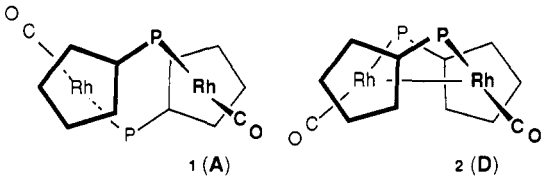

Figure 1. Schematic view of the complexes 1 and 2 emphasizing the configurational change from A to D.

appears as a facile metal–metal bond formation (or cleavage) process implying a drastic conformational change of the structure (Figure 1).

Figure 1 also schematizes another salient feature of the transformation: it shows that the metal–metal bond formation forces the two carbonyl ligands occurring in a transoid position in 1 to adopt a cisoid position in 2. Moreover, mimicking a continuous pathway from 1 to 2 (and return) is easy, using a ball and stick molecular model, essentially by combining rotations around the Rh–*Cp*, C_{Cp}–P, and P–Rh axes (*Cp* is the centroid of the cyclopentadienyl ring). This led us to postulate an intramolecular process without any requirement of a dissociation of the dinuclear structure; therefore an electrochemical study was undertaken.

Many compounds displaying reversible rearrangements upon charge transfer have long been known,[2a-d] and redox-induced structural changes have been recently reviewed by Geiger.[2b] In particular, various geometric rearrangements or "isomerizations" occurring upon either reduction or oxidation of polymetallic complexes have been also described.[2c] Concerning dinuclear rhodium compounds, the most relevant electrochemical studies have been by Bard et al.[3a] and have shown that the phosphido-bridged homometallic complex $[Rh(\mu\text{-}tBu_2P)(CO)_2]_2$ undergoes an ECE type reduction—i.e., a chemical reaction between two-electron-transfer reactions—to form a dianion. In this case, the chemical step is a geometric isomerization occurring between two monoanionic intermediates characterized respectively by tetrahedral or square planar geometry around each metal atom. The heterometallic $[(CO)_2(PMe_3)Fe(\mu_2\text{-}tBu_2P)(\mu_2\text{-}CO)Rh(PMe_3)L]$ (*Fe–Rh*) complex also exhibits an ECE mechanism.[3b]

Numerous examples of electrochemical studies concerning the cyclopentadienyl mononuclear complexes of group 9 metals have been reviewed by Connelly and Geiger.[2a,d] It is known that oxidation of mononuclear cyclopentadienyl complexes of the type $CpML_2$ (M = Co, Rh; L = carbonyl, phosphine) involves the formation of a 17-electron monocation.[4,5b,c,e,6] In some cases, both cobalt[4b,c] and rhodium[5c,e] radical cations have proved to be stable enough to be isolated or studied by ESR spectroscopy. Nevertheless in two cases, namely the rhodium complexes

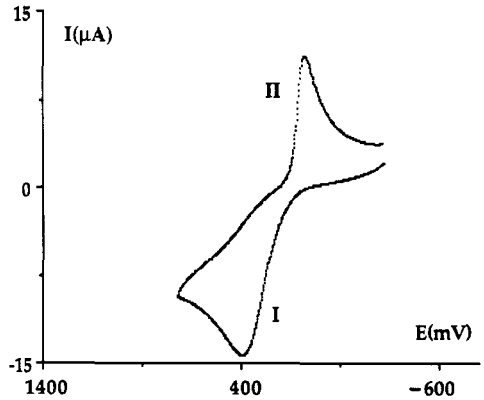

Figure 2. Cyclic voltammetry of $[Rh(\mu\text{-}C_5H_4PPh_2)(CO)]_2$ (1) 10^{-3} M in CH_2Cl_2–Bu_4NBF_4 (0.3 M) at a Pt electrode (1 mm) with scan rate 0.1 $V \cdot s^{-1}$.

$[CpRhL(PPh_3)]$, L = CO or PPh_3, chemical and electrochemical oxidations lead, through an only partly understood dimerization process,[2d] to the metal–metal-bonded dication of a fulvalene complex.[4a,5b,d] Formation of this dication by oxidation of the neutral dimetallic complex $[Rh_2(CO)_2(PPh_3)_2(\eta^5\text{:}\eta^5\text{-}C_{10}H_8)]$ has been shown to involve an ECE process where the intervening chemical step is a fast and reversible cis ↔ trans conformational change.[2b] In fact, several reports have generally shown that the coupling occurs through the ligands rather than through the metals.[7] Importantly, the orientation of this coupling toward carbon–carbon bond formation or toward metal–metal bond formation appears to be dependent on the nature of the phosphine: this has been shown in the one-electron oxidation of [CpRh(CO)L], L = PMe_3 or $P(OPh)_3$, which, in contrast to the previous cases, dimerizes through the metal,[8] this metal–metal bond formation involving coupling of two *positively charged* paramagnetic metal centers.

Preliminary observations on the electrochemistry of the present ((diphenylphosphino)cyclopentadienyl)rhodium redox system have already been described.[9] It is clear that the bridged structure prevents the coupling from occurring through the cyclopentadienyl ligands and therefore offers an interesting opportunity to further study the intimate mechanism of the metal–metal bond formation: does it involve coupling between two oxidized rhodium centers (EEC mechanism) or does the coupling occur after the uptake of the first electron (ECE mechanism)?

Results

A typical voltammogram at 0.1 $V \cdot s^{-1}$ for the oxidation of $[Rh(\mu\text{-}C_5H_4PPh_2)(CO)]_2$ (1) in CH_2Cl_2–Bu_4NBF_4 (0.3 M) at a Pt-disk electrode is shown in Figure 2. The first anodic scan shows only a single large oxidation wave, I, with an anodic peak potential Ep_I at 0.4 V. Upon scan reversal, a reduction wave, II, with a cathodic peak potential Ep_{II} at 0.08 V is observed. Bulk electrolysis controlled-potential coulometry experiments carried out at 0.5 V gave a dark red solution and an n_{app} value (faradays per mole of reactant consumed) of 2.3. The IR absorption of the electrolyte was monitored during the electrolysis; an

(2) (a) Connelly, N. G.; Geiger, W. E. *Adv. Organomet. Chem.* **1984**, *23*, 1–92. (b) Geiger, W. E. *Prog. Inorg. Chem.* **1985**, *33*, 275. (c) Geiger, W. E.; Connelly, N. G. *Adv. Organomet. Chem.* **1985**, *24*, 87–130. (d) Connelly, N. G. *Chem. Soc. Rev.* **1989**, *18*, 153–185.

(3) (a) Gaudiello, J. G.; Wright, T. C.; Jones, R. A.; Bard, A. J. *J. Am. Chem. Soc.* **1985**, *107*, 888–897. (b) Moulton, R. D.; Chandler, D. J.; Arif, A. M.; Jones, R. A.; Bard, A. *J. Am. Chem. Soc.* **1988**, *111*, 5714–5725.

(4) (a) McKinney, R. J. *J. Chem. Soc.* **1980**, 603–604. (b) McKinney, R. J. *Inorg. Chem.* **1982**, *21*, 2051–2056. (c) Harlow, R. J.; Mc Kinney, R. I.; Whitney, J. F. *Organometallics* **1983**, *2*, 1839–1842.

(5) (a) Connelly, N. G.; Lucy, A. R.; Galas, A. M. R. *J. Chem. Soc., Chem. Commun.* **1981**, 43–44. (b) Connelly, N. G.; Lucy, A. R.; Payne, J. D.; Galas, A. M. R.; Geiger, W. E *J. Chem. Soc., Dalton Trans.* **1983**, 1879–1885. (c) Connelly, N. G.; Freeman, M. J.; Manners, I.; Orpen, A. G. *J. Chem. Soc., Dalton Trans.* **1984**, 2703–2712. (d) Freeman, M. J.; Orpen, A. G.; Connelly, N. G.; Manners, I.; Raven, S. J. *J. Chem. Soc., Dalton Trans.* **1985**, 2283–2289. (e) Connelly, N. G.; Raven, S. J. *J. Chem. Soc., Dalton Trans.* **1986**, 1613–1718.

(6) Gennett, T.; Grzesczyk, E.; Jefferson, A.; Sidur, K. M. *Inorg. Chem.* **1987**, *26*, 1856–1860.

(7) Leading references may be found in ref 2d. Also see concerning polyolefin–cyclopentadienyl–cobalt complexes: Geiger, W. E.; Gennett, T.; Lane, G. A.; Salzer, A.; Rheingold, A. L. *Organometallics* **1986**, *5*, 1352–1359.

(8) Fonseca, E.; Geiger, W. E.; Bitterwolf, T. E.; Rheingold, A. L. *Organometallics* **1988**, *7*, 567–568.

(9) He, X. D.; Maisonnat, A.; Dahan, F.; Poilblanc, R. *Fourth European Symposium on Inorganic Chemistry*; DFG Ed.: Freiburg, Germany, 1988.

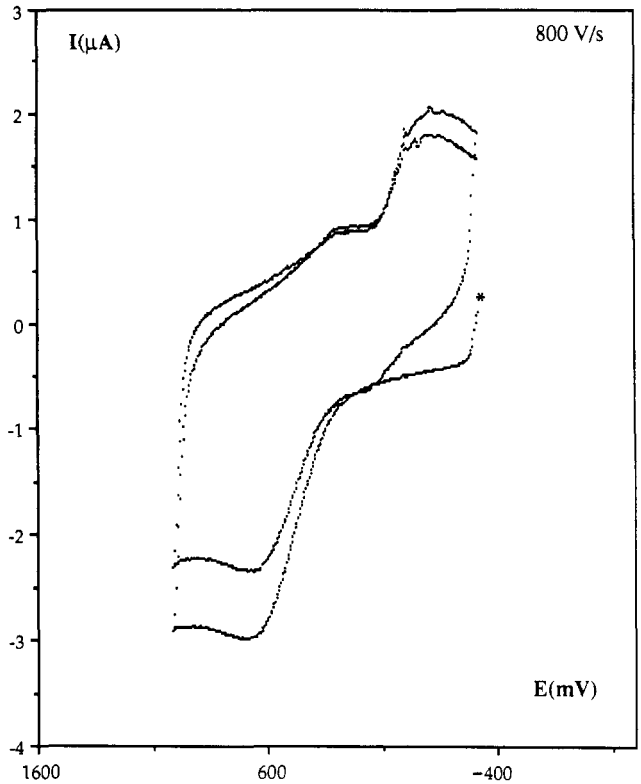

Figure 3. Experimental repetitive two-scan cyclic voltammogram of $[Rh(\mu\text{-}C_5H_4PPh_2)(CO)]_2$ (1) 10^{-3} M in CH_2Cl_2–Bu_4NBF_4 (0.3 M) at a Pt microelectrode (100 μm) with scan rate 800 $V \cdot s^{-1}$. An asterisk indicates the starting potential.

increase of the intensity of the band at 2084 cm^{-1} could be observed, providing evidence for the slow formation of the well-known dication $[Rh(\mu\text{-}C_5H_4PPh_2)(CO)]_2^{2+}$ (**2a**). As expected for such a diamagnetic compound, no ESR signal was observed from the resulting solution. Reduction of this solution at –0.3 V regenerated a light-orange solution, which, after consumption of 1.9 faradays/mol, exhibited a cyclic voltammetric behavior at 0.1 $V \cdot s^{-1}$ identical with the original one. This confirms that the system is overall chemically reversible, since 1 can be obtained by reduction of 2 and vice versa.[9] Nevertheless, two-scan repetitive cycle voltammograms clearly show that the system is complex. Figure 3 exemplifies this with such a two-scan voltammogram scanned at 800 $V \cdot s^{-1}$.

In order to elucidate the mechanism of oxidation, we resorted to simulation of fast cyclic voltammetry at a microelectrode.[10-12] Figure 4 shows a series of experimental cyclic voltammograms observed when the potential is repetitively scanned (stationary-state behavior) between –0.32 V (starting potential) and 1.02 V at a 100-μm platinum electrode. In this series, all the first cyclic voltammograms (not represented in Figure 4 for clarity) were apparently similar to those previously shown in Figure 3. In Figure 4, the cyclic votammograms show that when the

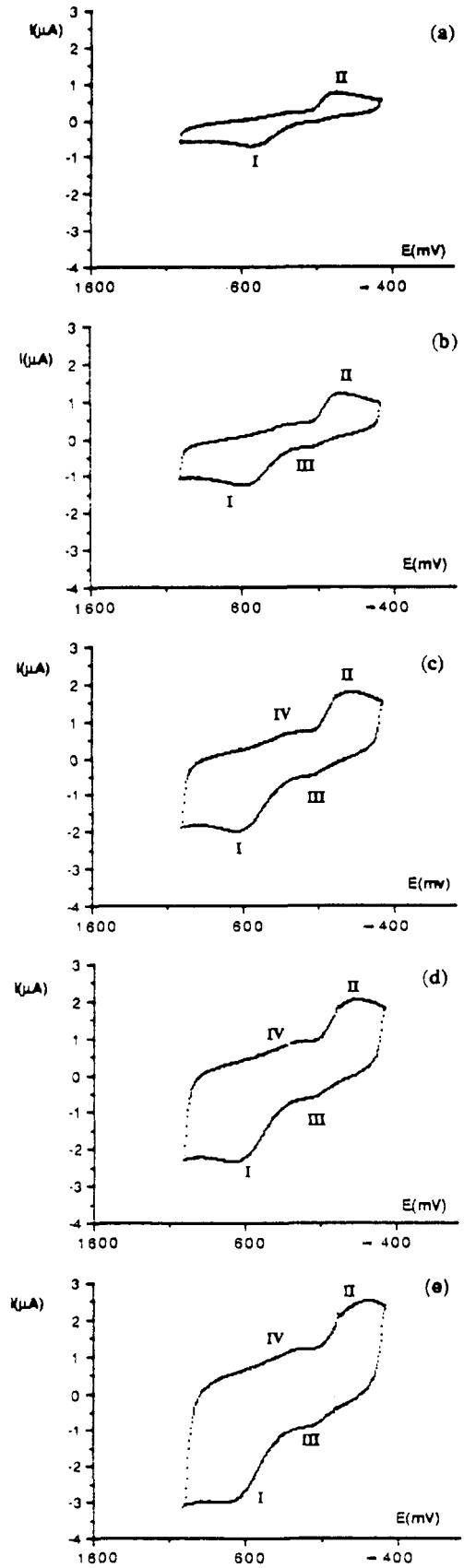

Figure 4. Expermental cyclic voltammograms obtained after repetitive scans (stationary state) for $[Rh(\mu\text{-}C_5H_4PPh_2)(CO)]_2$ (1) 10^{-3} M in CH_2Cl_2–Bu_4NBF_4 (0.3 M) at a Pt microelectrode (100 μm) with the following scan rates ($V \cdot s^{-1}$): (a) 100; (b) 300; (c) 600; (d) 800; (e) 1200.

scan rate is made increasingly large, a new oxidation wave, III, develops in the potential range 0.1–0.15 V ($100 \leq v \leq 1200$ $V \cdot s^{-1}$). Note that wave III is only barely observable

(10) Even if the currents of capacitive origin represent the main components in experimental cyclic voltammograms at high scan rates, these were not simulated or reported in the simulations. Incorporation of a "blank" capacitive current, measured prior to addition of the rhodium complex, to the simulated Faradaic currents (or the equivalent subtraction of this blank capacitive current to the experimental voltammograms) would be of little help, if not misleading, since this blank capacitive current would never be identical to the capacitive component in the presence of a Faradaic contribution. This is all the more true when dealing with stationary-state voltammograms.

(11) (a) Gosser, D. K.; Rieger, P. H. *Anal. Chem.* **1988**, *60*, 1159–1167. (b) Gosser, D. K., Jr.; Zhang, F. *Talanta* **1991**, *38*, 715–722.

(12) Fleischmann, M.; Pons, J.; Rolison, D. R.; Smidt, P. P. In *Ultramicroelectrodes*; Datatech Systems Inc.: Morganton, NC, 1987.

on the second voltammogram reported in Figure 4. Similarly, a second reduction peak, IV ($Ep \sim 0.18$ V), is also observed in the reductive scans. Such a behavior is fully consistent with the occurence of an ECE mechanism involving two redox couples A/B (waves I/IV) and C/D (waves III/II) linked by a B/C chemical step, as outlined in Scheme I, where A and D represent compounds 1 and 2, respectively.

Scheme I

$$A \rightleftarrows B + e^- \quad E^\circ_1, k^\circ_1, \alpha_1 \quad \text{"E"} \qquad (1a)$$

$$B \underset{k_{-1}}{\overset{k_1}{\rightleftharpoons}} C \qquad \text{"C"} \qquad (2a)$$

$$C \rightleftarrows D + e^- \quad E^\circ_2, k^\circ_2, \alpha_2 \quad \text{"E"} \qquad (3a)$$

Under such circumstances, when $E^\circ_1 > E^\circ_2$, and at small scan rates (Figure 2), wave I features the overall two-electron oxidation of A into the dication D. Reciprocally, the overall two-electron reduction of D into the neutral species A is observed at wave II. Shortening the time scale by increasing the scan rate ($v \geq 300$ V·s^{-1}) allows some of the one-electron reduction intermediate C to be oxidized at wave III before its complete conversion to species B. At even larger scan rates ($v > 600$ V·s^{-1}), partial reduction of the transient intermediate B can also be observed at wave IV. Starting from the appearance of a plateau shape in the voltammograms of Figure 4c and also 4d, the wave can be clearly seen with its maximum (peak shape) in voltammogram 4e at 1200 V·s^{-1}. By a decrease of the scan rate, the plateau shape disappears from voltammogram 4c to 4a.

To test the above mechanism quantitatively we resorted to simulation[11] of the Faradaic components of the voltammograms represented in Figure 4. The results of these simulations are shown in Figure 5 for the set of parameters indicated in Scheme II (see Experimental Section).

Scheme II

$$A \rightleftarrows B + e^- \quad E^\circ_1 = 0.40 \text{ V}, k^\circ_1 = 0.04 \text{ cm·s}^{-1}, \alpha_1 = 0.3 \qquad (1b)$$

$$B \underset{k_{-1}}{\overset{k_1}{\rightleftharpoons}} C \quad k_1 = 4000 \text{ s}^{-1}, k_{-1} = 2000 \text{ s}^{-1} \qquad (2b)$$

$$C \rightleftarrows D + e^- \quad E^\circ_2 = 0.05 \text{ V}, k^\circ_2 = 0.075 \text{ cm·s}^{-1}, \alpha_2 = 0.5 \qquad (3b)$$

Discussion

The most significant result to be considered here is the occurrence of two monocationic intermediates B and C. In the absence of other structural indications, the direct relationship of B to the neutral species A, and of C with the dicationic species D, strongly suggests similarities of the structures within each redox couple. In other words, the monocationic intermediates B and C are assumed to be respectively non-metal–metal-bonded and metal–metal-bonded complexes. The reversible chemical step of the ECE mechanism appears therefore as a metal–metal bond formation process upon oxidation (or breaking upon reduction). We have found no reason to consider more complicated processes. In particular, an oxidative coupling involving C–C bond formation[4a,5a] as observed with the monometallic related complex $[\eta^5\text{-}C_5H_5RhL(PPh_3)]$ (L = CO, PPh_3) would lead to some fulvalene derivative which is clearly not observed in the case of the present bridged bimetallic complexes.

The structures proposed for intermediates B and C are schematized in Figure 6, by supposing that they are strongly correlated with the fully described structures of A and D, respectively, compounds 1 and 2 (see also Figure 1). We assumed in particular, a transoid conformation of the CO ligands for B and a cisoid conformation for C. We present in the same figure four tentative MO diagrams,

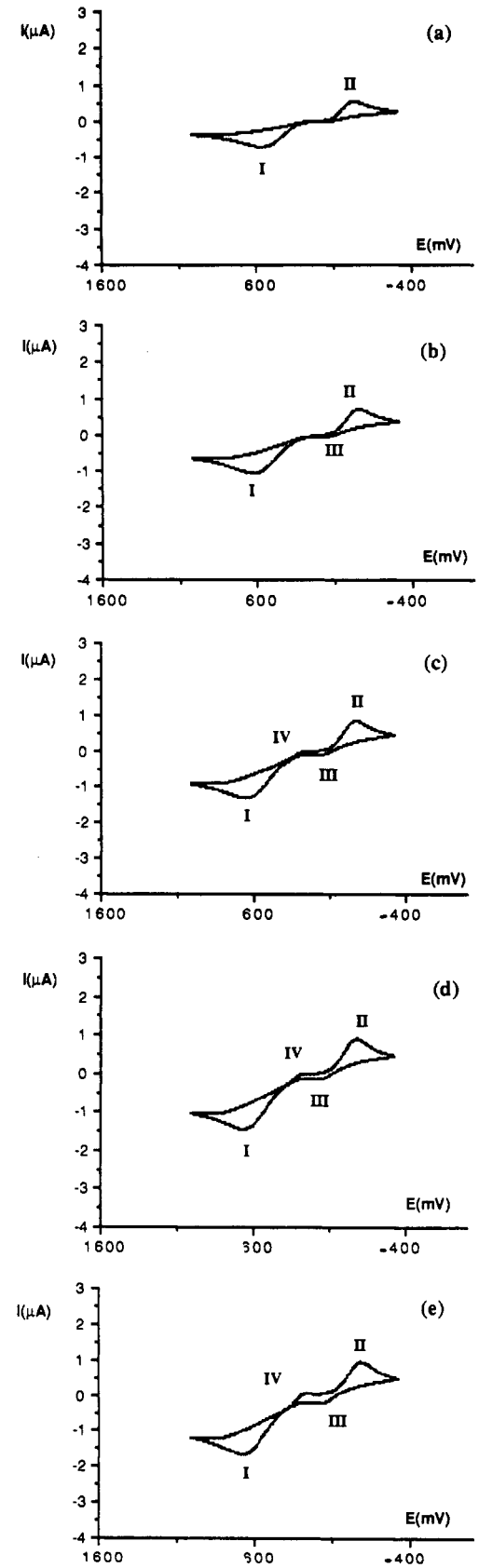

Figure 5. Simulated Faradaic voltammograms at various scan rates with the following scan rates (V·s^{-1}): (a) 100; (b) 300; (c) 600; (d) 800; (e) 1200. The voltammograms shown correspond to the second scan.

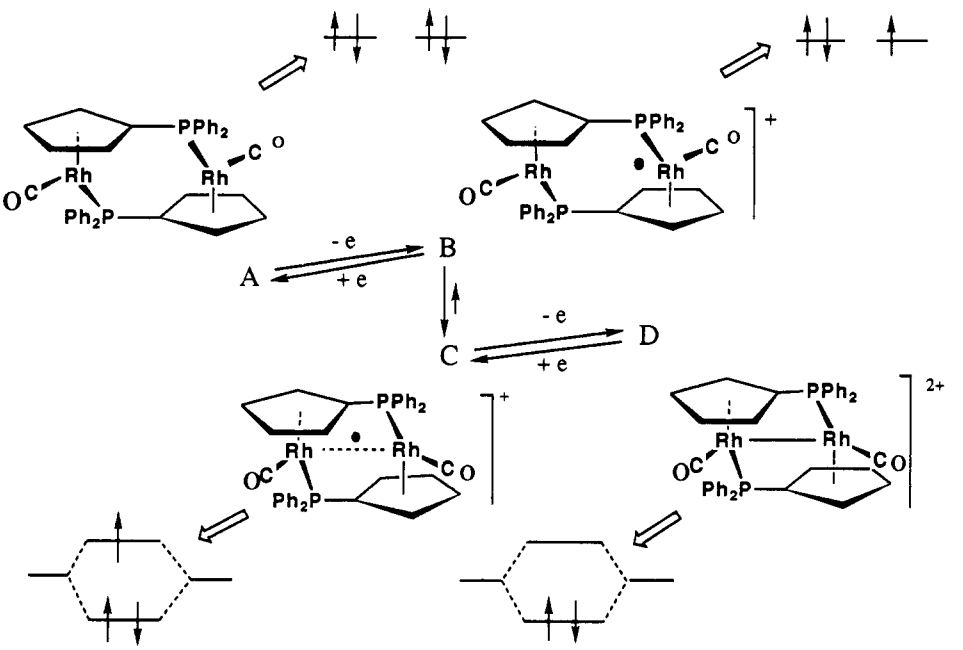

Figure 6. Proposed ECE mechanism and postulated structures of the concerned species A–D.

focusing on the HOMO's of the monometallic moieties when no metal–metal bond is involved (cases A and B) or correlating these d orbitals to the metal–metal bonding and antibonding orbitals when this bond is fully or partly formed in the dimetallic complexes (respectively bond order 1 in D and 0.5 in C). In $[\eta^5\text{-}C_5H_5Rh(CO)L]$ complexes, this HOMO orbital ($1b_1$) has been shown, from molecular orbital calculations[13,14,15b] and photoelectron spectroscopy data,[15a] to be an admixture of cyclopentadienyl e_1^+ and metal d_{xy}; it is oriented in the right direction to account for the M–M coupling. The already published—but not discussed—crystal structure data for the Rh^{II}–Rh^{II} metal–metal-bonded complexes **3–5**,[1i] and the data[8] for the nonbridged dication $[(\eta^5\text{-}C_5H_5)Rh(CO)(P(OPh)_3)]_2^{2+}$ (Figure 7), should also be considered from this point of view. In spite of the large diversity of these bridged and nonbridged structures, and also of the ligands, a coherent similarity in the angular partition of the ligands is observed; specifically, the pyramidalization at rhodium is remarkably constant along the series: it would enhance, in the dimetallic species, the bonding character of the orbital involved in the Rh···Rh interaction. Such a situation is expected to be also existing in the intermediate C.

Finally, intermediate B would therefore be described as a mixed-valence [Rh^{II}, Rh^{I}] complex and the intermediate C is supposed to present a three-electron metal–metal bond. It is significant that this proposal correctly rationalizes why this monocationic intermediate appears to be more easily oxidized ($E°_2$ = 0.05 V) than the neutral reduced complex A ($E°_1$ = 0.4 V), as the metal–metal interaction promotes the extra electron in a high-level antibonding orbital.

The previously described digital simulation shows that the expected ECE mechanism is in complete accordance with the experimental results. Note that since the potentials of two couples B/A and D/C are in order $E°_1$ > $E°_2$, one should consider the possible interference of a disproportionation reaction between species B and C:

$$B + C \rightarrow A + D \qquad (4)$$

However, including this extra reaction in the simulations led to no observable change of the simulated voltammograms, with respect to those presented in Figure 5. This is in agreement with the results of a previous theoretical analysis of the ECE/DISP (eqs 1–4) sequence.[16] Indeed, for an equilibrium constant close to unity (k_1/k_{-1}, for reaction 2) for the B/C chemical interconversion, the role of reaction 4 can be shown to be negligible even under conditions where its rate constant is close to the diffusion limit.

The derived rate constants k_1 and k_{-1} are extremely high (Scheme II): even higher than the data previously given

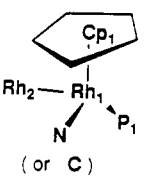

(or C)

Selected angles in :

* $[Rh^{II}(\mu\text{-}C_5H_4PPh_2)$ pyridine$]^{2+}$, 2

Rh(2)-Rh(1)-P(1)	77.37(5)
Rh(2)-Rh(1)-N(1)	101.8(2)
Rh(2)-Rh(1)-*Cp*(1)	110.4(2)
P(1)-Rh(1)-N(1)	92.3(2)
P(1)-Rh(1)-*Cp*(1)	132.4(2)
N(1)-Rh(1)-*Cp*(1)	128.7(2)

* $[(CH_3)Rh^{II}(\mu\text{-}C_5H_4PPh_2)_2Rh^{II}(I)]$, 5

Rh(2)-Rh(1)-*Cp*(1)	125.5(1)
P(1)-Rh(1)-C(1)	87.0(3)
P(1)-Rh(1)-*Cp*(1)	126.3(3)
C(1)-Rh(1)-*Cp*(1)	141.3(1)
Rh(2)-Rh(1)-P(1)	79.10(5)
Rh(2)-Rh(1)-C(1)	94.8(3)

* $[(COCH_3)Rh^{II}(\mu\text{-}C_5H_4PPh_2)_2Rh^{II}(CO)]^+$, 4

Rh(2)-Rh(1)-*Cp*(1)	108.2(2)
P(1)-Rh(1)-C(1)	93.1(2)
P(1)-Rh(1)-*Cp*(1)	133.9(2)
C(1)-Rh(1)-*Cp*(1)	131.4(2)
Rh(2)-Rh(1)-P(1)	76.84(4)
Rh(2)-Rh(1)-C(1)	91.7(2)

* $[CpRh^{II}(CO)P(OPh)_3)]_2^{2+}$

Rh(2)-Rh(1)-*Cp*(1)	117.8(6)
P(1)-Rh(1)-C(1)	89.8(4)
P(1)-Rh(1)-*Cp*(1)	128.6(3)
C(1)-Rh(1)-*Cp*(1)	126.8(6)

Figure 7. Angular partitions of the ligands around rhodium in the complexes **3–5** (from ref 1i) and $[CpRh(COP(OPh)_3)]_2^{2+}$ (from ref 8). *Cp*(1) represents the centroid of the cyclopentadienyl rings. The angles Rh(2)–Rh(1)–*Cp*(1) have been oriented in the same way in the four cases.

(13) Schilling, B. E. R.; Hoffmann, R.; Lichtenberger, D. L. *J. Am. Chem. Soc.* **1979**, *101*, 585–598.
(14) Hofmann, P.; Padmanabhan, M. *Organometallics* **1983**, *2*, 1273–1284.
(15) (a) Lichtenberger, D. L.; Blevins, C. H.; Ortega, R. B. *Organometallics* **1984**, *3*, 1614–1622. (b) Lichtenberger, D. L.; Calabro, D. G.; Kellogg, G. E. *Organometallics* **1984**, *3*, 1623–1630.
(16) Amatore, C.; Savéant, J.-M. *J. Electroanal. Chem.* **1979**, *102*, 21–40.

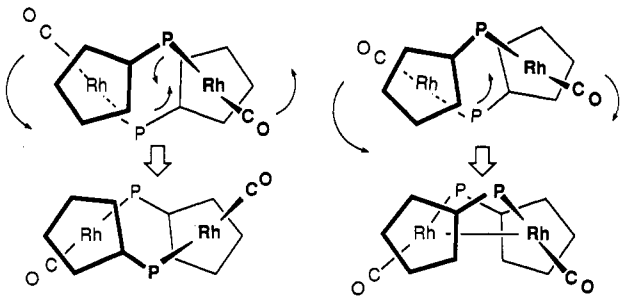

Figure 8. Conrotatory and disrotatory deformations of the $[M(\mu\text{-}C_5H_4PPh_2)]_2$ unit.

for analogous rhodium compounds.[3a] The small value of the equilibrium constant k_1/k_{-1}, near 2, probably reveals a close adjustment between the exergonic effect of the metal–metal bond formation and the endergonic effect of the conformational change ($\Delta G_{B/C} \sim 0.5$ kcal·mol^{-1}).

Interestingly, it has been observed that, on the NMR time scale, the dimetallic neutral species **1** exhibits a plane of symmetry and a 2-fold axis in addition to the center of symmetry present in the crystal.[1d] This observation has be interpreted in terms of intramolecular wagging of the molecule around a mean plane. In that case, this interconversion has been assumed to be of low activation energy, the ^{1}H NMR spectra being unchanged in the temperature range −70 to +30 °C at 250 MHz. Indeed, this energy barrier is probably less than 5 kcal·mol^{-1} for a pathway which we described as a *conrotatory deformation* (Figure 8). From this point of view, the B → C configurational change is the result of a *disrotatory deformation* of the same bridging unit and its high rate could be again a proof of the very high flexibility of the $[Rh(\mu\text{-}C_5H_4PPh_2)]_2$ bridging unit.

It would also be interesting to understand why, in spite of the charges of the involved species, the value of k°_2 is almost twice that of k°_1. In the absence of other information, we are tempted to correlate this unexpected difference to the type of structures involved respectively in the redox couples A/B and C/D, the second being more suitable for a closer approach of the metal orbitals toward the electrode.

As a conclusion, it is proposed to generalize the hypothesis of an ECE mechanism also to the oxidative metal–metal coupling of the 18-electron mononuclear [CpRh(CO)L] complexes considered in the Introduction.[8] Instead of admitting the occurrence of a reaction between *two cationic* species—a kinetically unfavored process—it could be suggested in these cases that the oxidized 17-electron monocationic species could be the target of fast nucleophilic attack by the neutral species, *in a* configuration *close to* that of B, leading to an easily oxidizable 17e/18e C type precursor. In other words, the 17e/17e intermediate may not be accessible in all the cases where some electronic communication between the metal centers (whether this is purely electrostatic, a through-bond effect, or a combinaison of the two)[17] appears in the 17e/18e precursors. In such case, the ECE mechanism would be more efficient than an EEC mechanism.

(17) We thank one of the reviewers for suggesting that the interaction in the postulated 17e/18e intermediate could be not only a through metal–metal bond effect between two monometallic species but also an electrostatic effect. He also suggested that, in the mononuclear systems, the two radical cations being generated at the same potential make the 17e/17e precursor readily available in contrast with the present studied case, in which the 17e/18e intermediate is necessarily formed as a consequence of the dimetallic structure. Therefore, in the monometallic case, from our point of view, the ECE or EEC nature of the oxidative process could be beyond the control of the relative probabilities of the encounters, either of two cationic radicals or of one cationic radical with a neutral species initially present in the vicinity of the electrode.

Experimental Section

Chemicals. The compounds $[Rh(\mu\text{-}C_5H_4PPh_2)(CO)]_2$ (**1**) and $[Rh(\mu\text{-}C_5H_4PPh_2)(CO)_2]^{2+}(X^-)_2$ (X = BF_4^- (**2a**), PF_6^- (**2b**)) were prepared according to published procedures.[1b]

Dichloromethane, CH_2Cl_2 (SDS, purex), was passed through an activated alumina column prior to use, and the solutions were deaerated by means of bubbling argon for 10 min prior to the measurements. The supporting electrolyte Bu_4NBF_4 ($TBABF_4$, Aldrich analytical grade) was used as received.

Electrochemical Studies. All electrochemical experiments were performed in methylene chloride because **2** was known to form solvato complexes $[Rh(\mu\text{-}C_5H_4PPh_2)(Solv)]^{2+}$ in coordinating solvents like tetrahydrofuran and acetonitrile.[1e]

Electrochemical measurements were carried out with a homemade potentiostat using an interfacing hardware with microcomputer PC compatible. Positive feedback (scan rate > 1 V·s^{-1}) or the interrupt method (scan rate < 1 V·s^{-1}) was used to compensate for *IR* drop. Electrochemical experiments were performed in an airtight three-electrode cell connected to a vacuum/argon line. The cell was degassed and filled according to standard vacuum techniques. The reference electrode consisted of a SCE separated from the solution by a bridge compartment filled with the same solvent and supporting electrolyte solution as used in the cell. The counter electrode was a spiral of ca. 1 cm^2 apparent surface area, made from a length of ca. 8 cm of a 0.5-mm-diameter platinum wire. The working electrode was a 100-μm-diameter Pt disk, and the RDE (rotating disk electrode) was a 2 mm diameter Pt disk (Tacussel EDI). With the above reference and bridge system, E° = 0.54 V was obtained for 2 mM ferrocene solutions.

Digital Simulations. All the simulations of Faradaic currents were performed using a Pascal version of the "General Program of Simulation" kindly provided to us by Dr. D. Gosser (City College of the City University of New York)[11] and were run on a PC-286. The currents of capacitive origin were not simulated although they represent the main component in cyclic voltammetry at large scan rates.

To initiate the simulations a complet set of reasonable values for the potentials E°_1 and E°_2, the standard heterogeneous rate constants k°_1 and k°_2, the chemical rate constants k_1 and k_{-1}, the charge-transfer coefficients α_1 and α_2, and the diffusion coefficients D must be assumed. This set of initial values was selected as follows.

The potential E°_2 was approximated as the average of Ep_{II} and Ep_{III} for the C/D couple, i.e. 0.043 V, and E°_1, as the average of Ep_I and Ep_{IV} at 800 V·s^{-1} for the couple A/B, i.e. 0.45 V. k°_2 determined by the Nicholson and Shain method[18] was 0.1 cm·s^{-1}; from the Butler–Volmer equation[19] k°_1 was determined as 1.1 × 10^{-3} cm·s^{-1} (without considering any follow-up chemical reaction). The charge-transfer coefficients α_1 and α_2 were estimated from the half-width of the wave ($Ep - Ep/2 = 47.7/\alpha n$)[19] for a quasi-reversible system, and the values of the parameters α_1 and α_2 so obtained by this method were compared with those determined from the graph of $Ep = f(\log v)$. The values were chosen as the average values of the two methods: $\alpha_2 = 0.5$ and $\alpha_1 = 0.3$. Last, the value $D = 10^{-5}$ cm^2/s was retained for the diffusion coefficient.

Digital simulations were then optimized in three steps: (i) A digital simulation of the couple A/B and of the reaction B → C was performed by varying the parameters k_1, and then E°_1, α_1, and k°_1, until the best fit to the experimental voltammograms was reached. (ii) A digital simulation of the couple C/D and of the reaction C → B was performed under the same conditions as in (i). (iii) Finally, with coverage of the entire potential range, −0.32 to 1.02 V, by combination of the two sets of parameters obtained separately by (i) and (ii), a global digital simulation of the ECE mechanism was attempted. The overall process was then optimized until the best fit with the experimental voltammograms was reached.

Note that since electrochemical behavior depends on dimen-

(18) Nicholson, R. S. *Anal. Chem.* **1965**, *37*, 1351–1355. Nicholson, R. S.; Shain, I. *Anal. Chem.* **1964**, *36*, 706–723.

(19) Bard, A. J.; Faulkner, L. R. *Electrochemical Methods*; Wiley: New York, 1980.

sionless parameters such as $\lambda = k(RT/Fv)$, the sensitivity of determinations of k values is reflected by the changes of voltammograms in Figure 5 when the scan rate is modified.

Acknowledgment. This work was supported in parts by the CNRS [UPR 8241 (Toulouse) and URA 1110 (Paris)], Université Paul Sabatier (Toulouse), and Ecole Normale Supérieure (Paris).

OM920359Z

Synthesis, Reactivity, and Structure of Four-Coordinate (Vinylvinylidene)- and Five- and Six-Coordinate Enynyl(hydrido)rhodium Complexes with $[RhCl(P^iPr_3)_2]$ as a Molecular Unit†,1

Thomas Rappert, Oliver Nürnberg, Norbert Mahr, Justin Wolf, and Helmut Werner*

Institut für Anorganische Chemie der Universität Würzburg, Am Hubland, D-8700 Würzburg, Germany

Received June 29, 1992

The reaction of $[RhCl(C_8H_{14})_2]_2$ (**4**) with P^iPr_3 and enynes $HC{\equiv}CC(R){=}CH(R')$ [R = R' = H; R = CH_3, R' = H; R = H, R' = OCH_3] leads to the formation of either (enyne)- or enynyl(hydrido)rhodium complexes (**5a,b, 6c**) as the first isolable products. At 25–45 °C in toluene, *trans*-$[RhCl(HC{\equiv}CC(R){=}CH_2)(P^iPr_3)_2]$ (**5a,b**) and $[RhH\{C{\equiv}CCH{=}CH(OCH_3)\}Cl(P^iPr_3)_2]$ (**6c**) smoothly rearrange to give the isomeric (vinylvinylidene)rhodium derivatives *trans*-$[RhCl\{{=}C{=}CHC(R){=}CH(R')\}(P^iPr_3)_2]$ (**7a–c**) in nearly quantitative yield. The parent complex **7a** (R = R' = H) has also been prepared from **4**, P^iPr_3, and the alkynol $HC{\equiv}CCH(CH_3)OH$ via the substituted rhodium vinylidene complex *trans*-$[RhCl\{{=}C{=}CHCH(CH_3)OH\}(P^iPr_3)_2]$ (**9**), which undergoes elimination of water on treatment with acidic Al_2O_3 or traces of HX. Both **5a,b** and **6c** as well as the vinylvinylidene complexes **7a–c** react with pyridine at room temperature to give the octahedral rhodium(III) compounds $[RhH\{C{\equiv}CC(R){=}CH(R')\}Cl(py)(P^iPr_3)_2]$ (**11a–c**). In contrast, the reaction of **7b** with CO affords, instead of $[RhH\{C{\equiv}CC(CH_3){=}CH_2\}Cl(CO)(P^iPr_3)_2]$, the four-coordinate carbonyl complex *trans*-$[RhCl(CO)(P^iPr_3)_2]$ (**13**) and free enyne $HC{\equiv}CC(CH_3){=}CH_2$. Protonation of **7b** with HBF_4 gives the cationic carbyne rhodium derivative *trans*-$[RhCl\{{\equiv}CCH{=}C(CH_3)_2\}(P^iPr_3)_2]BF_4$ (**14**), which on treatment with NaH re-forms the vinylvinylidene compound **7b**. The molecular structures of **7b** and **11b** have been determined. Crystallographic data are as follows: **7b**, monoclinic space group $P2_1/c$ (No. 14) with a = 8.117 (3) Å, b = 38.946 (9) Å, c = 17.597 (6) Å, β = 93.99 (1)°, V = 5590 Å^3, and Z = 8; **11b**, triclinic space group $P\bar{1}$ (No. 2) with a = 9.3103 (5) Å, b = 11.7936 (8) Å, c = 15.322 (2) Å, α = 93.246 (7)°, β = 92.832 (6)°, γ = 108.981 (5)°, V = 1584 Å^3, and Z = 2.

Introduction

Transition-metal complexes containing vinylvinylidenes as ligands belong to a type of compound in which a conjugated and a cumulated double-bond system is combined in the same molecule. Complexes of the general composition **1** have previously been obtained from a labile precursor such as $[Cr(CO)_5(OEt_2)]$ and an activated alkyne, e.g., $HC{\equiv}CCO_2Me$,[2] or by formal insertion of $C_2(CO_2Me)_2$ into the C_α–C_β bond of a vinylidene–metal unit.[3] Vinylacetylene, $HC{\equiv}CCH{=}CH_2$, or derivatives thereof have as far as we know not been used as starting materials for compounds of type **1**, which could be due first to the sophisticated methods of synthesis and second to the sensitivity toward polymerization of these substances. Recently, Devanne and Dixneuf used vinylacetylenes in the presence of ROH to prepare (alkenylcarbene)ruthenium complexes and concluded that the substituted carbene moieties were formed via nucleophilic attack of the alcohol on vinylvinylidene ligands.[4]

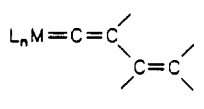

1

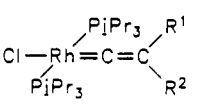

2

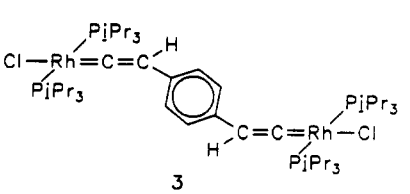

3

Scheme I

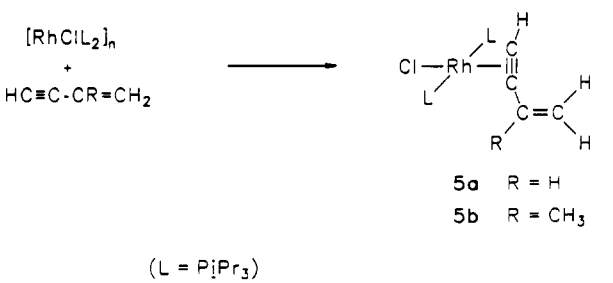

† Dedicated to Professor Lord Lewis on the occasion of his 65th birthday.

(1) Part 21 of the series Vinylidene Transition-Metal Complexes. For part 20, see: Werner, H.; Schwab, P.; Mahr, N.; Wolf, J. *Chem. Ber.*, in press.

(2) Berke, H.; Härter, P.; Huttner, G.; Zsolnai, L. *Z. Naturforsch., B: Anorg. Chem., Org. Chem.* **1981**, *36*, 929–937.

(3) Gamble, A. S.; Birdwhistell, K. R.; Templeton, J. L. *Organometallics* **1988**, *7*, 1046–1050.

0276-7333/92/2311-4156$03.00/0